

Article ID: 1007-4627(2012)04-0353-05

Thermal Dilepton Production in the Expanding QGP

FU Yong-ping, YANG Guang-di, XI Qin

(Department of Physics and Mathematics, Lincang Teachers College, Lincang 677000, Yunnan, China)

Abstract: The secondary thermal dileptons produced from the quark-gluon plasma are investigated. The secondary thermal dileptons produced at RHIC energy were concentrated in the low mass region of $0.2 \text{ GeV} < M < 0.8 \text{ GeV}$. The mechanism of the secondary thermal dileptons could be properly explained the enhancement of the dilepton yield in PHENIX experiments for Au-Au 200 AGeV collisions. For Pb-Pb 5.5 ATeV collisions at LHC, the enhancement is more evident in the low mass region of $0.3 \text{ GeV} < M < 1.0 \text{ GeV}$, and also exists in the intermediate mass region of $1.0 \text{ GeV} < M < 2.5 \text{ GeV}$ at LHC.

Key words: dilepton production; secondary thermal dilepton; relativistic heavy ion collision

CLC number : O572.2 **Document code :** A

1 Introduction

Because the mean free path of virtual photons is large compared with the size of the QGP, it is relatively easy to probe the thermal dilepton emitted from the hot QGP^[1-3] for studying QGP property. However, so far no evident experiments show that any information about the thermal dilepton is exactly produced from the QGP. In the theory of the phase transition, thermal dileptons are dominant in the intermediate mass region between the ψ and the J/Ψ vector meson^[4-7].

The measurement of the dilepton continuum at Relativistic Heavy Ion Collider (RHIC) was performed by the PHENIX experiments for Au-Au 200 AGeV collisions^[8-9]. The experiments have observed an excess of dilepton yield over the hadronic decays by a factor $2 \sim 3$ for masses between 0.2 and 0.8 GeV. Such phenomena were found at Super Proton Synchrotron (SPS), the enhancement of the dilepton yield was interpreted by chiral

symmetry restoration of meson decays in the hot medium, but such modifying scenarios could not properly explain the enhancement in Au-Au collisions at RHIC^[10-14].

In the present work, we investigate the secondary thermal dileptons (sec-th dileptons) produced from the hot QGP in the low mass region. The contribution of the thermal dileptons at low mass is covered by the cocktail of hadron decays. However, because the thermal partons are abundant in the low transverse momentum, the sec-th dilepton production turns into an important source at low mass. In the space-time evolution, the spectrum of sec-th dileptons produced by the annihilation of quarks and antiquarks in medium enhances the thermal spectrum in the low mass region of $0.2 \text{ GeV} < M < 0.8 \text{ GeV}$, and the enhancement in this mass region is a factor of $1 \sim 3$. The enhanced effect of sec-th dileptons at low mass can properly interpret the enhancement of the dilepton yield at

Received date: 10 May 2012; **Revised date:** 21 Jun. 2012

Foundation item: Scientific Research Foundation of Education Department of Yunnan Province (2012Y274); Supporting Science Foundation for High-level Talents Introduction of Lincang Teachers College (2012)

Biography: FU Yong-ping(1983-), male (Yi Nationality), Lincang, Yunnan, Doctor, working on the field of nuclear and particle physics; E-mail: yunfyp@sina.cn

RHIC for Au-Au 200 AGeV collisions.

According to the analysis of the space-time evolution, we discuss the enhancement of the dilepton yield at Large Hadron Collider (LHC) for Pb-Pb 5.5 ATeV collisions, the enhancement with a factor of $1 \sim 4$ is remarkable in the low mass region of $0.3 \text{ GeV} < M < 1.0 \text{ GeV}$. Furthermore, we find that the enhancement also exists in the intermediate mass region of $1.0 \text{ GeV} < M < 2.5 \text{ GeV}$, and the enhanced factor is almost $1 \sim 2$.

2 Thermal dilepton production

2.1 Expansion of hot quark-gluon system

When the QGP phase transforms to the mixed phase at the critical time τ_c , the balance of standard entropy and the fraction $f(\tau)$ of quark-gluon matter is given by^[15]

$$\frac{S_{\text{tot.}}(\tau)}{V(\tau)} = f(\tau)s_{\text{QGP}}(T_c) + (1 - f(\tau))s_{\text{HG}}(T_c), \quad (1)$$

where s_{QGP} and s_{HG} denote the entropy density of the QGP phase and the hadronic phase, respectively. $S_{\text{tot.}}(\tau)$ is the total entropy, T_c is critical temperature.

In Eq. (1), the accelerating expanding volume of the cylindrical hydrotype is^[16]

$$V(\tau) = 2 \left(z_0 + v_z \tau + \frac{1}{2} a_z \tau^2 \right) \pi \left(R_0 + \frac{1}{2} a_{\perp} \tau^2 \right)^2. \quad (2)$$

The longitudinal value z_0 equals to the formation time. R_0 corresponds to the initial radius of the QGP system, it was chosen as $R_0 : 7 \text{ fm}$ (RHIC) and $R_0 : 11 \text{ fm}$ (LHC)^[17]. After expanding the terms of Eq. (2), it can be written as $V(\tau) = V_0 + \sigma\tau + a_v\tau^2 + O(\tau^3, \tau^4, \tau^5, \tau^6)$, where $V_0 = 2\pi R_0^2 z_0$, $\sigma = 2\pi v_z R_0^2$ and $a_v = \pi R_0^2 a_z + 2\pi R_0 z_0 a_{\perp}$. The values of the longitudinal acceleration a_z and transverse acceleration a_{\perp} are smaller than the value of the longitudinal velocity v_z . These accelerations are adjusted to the final conditions of flow velocities^[16]. A pure longitudinal expansion according to

the boost-invariant hydrodynamics of Bjorken represents a very useful approximation. Further research realizes that the transverse expansion of the plasma is of importance towards the later stages of the dynamics. When the transverse flow of the system is accounted for, it is found that the dilepton having their origin in hadronic matter are comparable to those originating in the QGP for large transverse momentum region^[18].

2.2 Thermal dilepton production

We briefly recall the production rate of thermal dileptons from the processes of annihilation $q\bar{q} \rightarrow 1^+1^-$. The thermal dilepton yield can be written as following^[15]

$$\frac{dN_{1^+1^-}^{\text{th}}}{dMdy} = \sum_q \sigma_{q\bar{q}}(M) \left[\int_{\tau_0}^{\tau_c} d\tau V(\tau) F(T) + F(T_c) \int_{\tau_c}^{\tau_h} d\tau f(\tau) V(\tau) \right], \quad (3)$$

where the mean cross section of $q\bar{q} \rightarrow 1^+1^-$ is $\sigma_{q\bar{q}} = 4\pi\alpha^2 e_q^2 / 9M^2$, and the integration factor is

$$F(T) = \frac{12K}{(2\pi)^4} M^3 T \sqrt{\frac{\pi MT}{2}} e^{-M/T}, \quad (4)$$

To consider the higher-order correction of $q\bar{q} \rightarrow 1^+1^-$, we use the K -factor as $K = 1 + 3\alpha_s$ ^[15]. In the above integration, the formation time τ_0 depends on the initial condition of the collisions, and the critical time is $\tau_c = (T_0/T_c)^3 \tau_0$. We chose the initial temperature as $T_0 = 370 \text{ MeV}$ for RHIC and $T_0 = 845 \text{ MeV}$ for LHC, and the critical temperature is chosen as $T_c = 160 \text{ MeV}$ ^[19–20].

The first term and second term of Eq. (3) correspond to the production rate of thermal dileptons in the QGP phase and the mixed phase, respectively. If $\sigma \gg V_0$ and a_v , the integration of the first term in Eq. (3) can be turned out an analytic result in the following^[15–16]

$$\frac{dN_{1^+1^-}^{\text{QGP}}}{dMdy} = \frac{9}{5} \left(\frac{\alpha R_0}{\pi} \right)^2 \frac{(\tau_0 T_0^3)^2}{M^3} \times K \left[H\left(\frac{M}{T_0}\right) - H\left(\frac{M}{T_c}\right) \right], \quad (5)$$

where the function $H(x) = x^2(8+x^2)K_0(x) + 4x(4+x^2)K_1(x)$, and $K_i(x)$ is the Bessel function.

The integration of the second term in Eq. (3) also can be done, the production rate of thermal dileptons from the mixed phase is

$$\frac{dN_{l^+l^-}^{\text{mix}}}{dMdy} = \sum_q \sigma_{q\bar{q}}(M)F(T_C)I(T_C), \quad (6)$$

where

$$I(T_C) = \int_{\tau_C}^{\tau_h} f(\tau)V(\tau)d\tau.$$

In the mixed phase, the fraction of the quark-gluon matter is

$$f(\tau) = \frac{g_{\text{QGP}}\left(\frac{\tau_C}{\tau}\right)^{4/3} - g_{\text{HG}}}{g_{\text{QGP}} - g_{\text{HG}}},$$

here the degeneracy of the QGP phase is $g_{\text{QGP}} = 37$, and the degeneracy of the hadronic gas is $g_{\text{HG}} = 3^{[2]}$. The production rate of thermal dileptons from the mixed phase is relatively small, because the system temperature of mixed phase is keeping at the relatively low T_C .

2.3 Secondary thermal dilepton production in the expanding QGP

In the hot and dense medium thermal partons interact with each other by the interaction of $q\bar{q} \rightarrow q'q'$, $g\bar{g} \rightarrow q'\bar{q}'$, and $q\bar{g} \rightarrow q'g$. Then the quark q' can convert into a dilepton by reacting with the anti-quark \bar{q}' ($q'\bar{q}' \rightarrow l^+l^-$). The production rate of the sec-th dileptons in the quark-gluon medium is given by

$$\frac{dN_{l^+l^-}^{\text{sec-th}}}{dM d^4x} = \sum_q \frac{\sigma_{q\bar{q}}(M)M^3}{(2\pi)^4} \int dE_1 dE_2 f'_1(E_1) f'_2(E_2), \quad (7)$$

where $f'_i(E_i)$ is the distribution of the secondary parton q' (\bar{q}'). According to Eq. (3), the distribution can be written as

$$f'(E) = \sum_q \int dM \int_{\tau_0}^{\tau_C} d\tau \sigma_P(M, T) V(\tau) F(T) + \sum_q \int dM F(T_C) \sigma_P(M, T_C) \int_{\tau_C}^{\tau_h} d\tau f(\tau) V(\tau). \quad (8)$$

In Eq. (8), the scattering channel σ_P includes: $q_1\bar{q}_1 \rightarrow q_2\bar{q}_2$, $q_1q_2(q_1\bar{q}_2) \rightarrow q_1q_2(q_1\bar{q}_2)$, $q_1q_1 \rightarrow q_1q_1$, $q_1\bar{q}_1 \rightarrow q_1\bar{q}_1$, $g\bar{g} \rightarrow q\bar{q}$, $q\bar{g} \rightarrow qg$. The mean cross sections of these scattering are calculated as following

$$\sigma_P(q_1\bar{q}_1 \rightarrow q_2\bar{q}_2) = \frac{8}{27} \frac{\pi\alpha_s^2}{s}, \quad (9)$$

$$\sigma_P(q_1q_2/q_1\bar{q}_2 \rightarrow q_1q_2/q_1\bar{q}_2) = \frac{8}{9} \frac{\pi\alpha_s^2}{s} \left(\ln \frac{\hat{s}}{m^2} + \frac{\hat{s}}{m^2} + \frac{1}{2} \right), \quad (10)$$

$$\sigma_P(q_1q_1 \rightarrow q_1q_1) = \frac{64}{27} \frac{\pi\alpha_s^2}{s} \ln \frac{\hat{s}}{m^2}, \quad (11)$$

$$\sigma_P(q_1\bar{q}_1 \rightarrow q_1\bar{q}_1) = \frac{16}{27} \frac{\pi\alpha_s^2}{s} \left(\ln \frac{\hat{s}}{m^2} + \frac{3}{2} \frac{\hat{s}}{m^2} + 1 \right), \quad (12)$$

$$\sigma_P(g\bar{g} \rightarrow q\bar{q}) = \frac{1}{3} \frac{\pi\alpha_s^2}{s} \left(\ln \frac{\hat{s}}{m^2} - \frac{7}{4} \right), \quad (13)$$

$$\sigma_P(q\bar{g} \rightarrow qg) = \frac{14}{9} \frac{\pi\alpha_s^2}{s} \left(\ln \frac{\hat{s}}{m^2} + \frac{9}{7} \frac{\hat{s}}{m^2} + \frac{1}{2} \right). \quad (14)$$

In the above calculations, the cutoff was chosen as $m^2 = 2\pi\alpha_s T^2/3^{[15]}$, m is the mass of a quark. For the convenience of the integration in Eq. (8), we divide the processes of sec-th dilepton production into two types: type I is the process which includes the scattering of $q_1\bar{q}_1 \rightarrow q_2\bar{q}_2$, and the corresponding cross section $\sigma_P(q_1\bar{q}_1 \rightarrow q_2\bar{q}_2)$ does not depend on the temperature. Type II denotes to the remaining scattering which depend on the temperature.

3 Numerical results

In Fig. 1, we plot the contribution induced by the sec-th dileptons at RHIC and LHC energies. Because the gluons are abundant at low energy state, the QCD processes including gluons are important at small mass region^[19]. Although the secondary parton distribution function is suppressed by a factor α_s^2 , the secondary scattering channels $g\bar{g} \rightarrow q\bar{q}$, $q\bar{g} \rightarrow qg$, $\bar{q}g \rightarrow \bar{q}g$ contain gluons in the secondary parton distributions, so the gluon abundance effect can enhance the contribution of these distribution functions at small mass. In

Fig. 1, the spectra of the sec-th production are important in the mass region of $0.3 \text{ GeV} < M < 0.5$

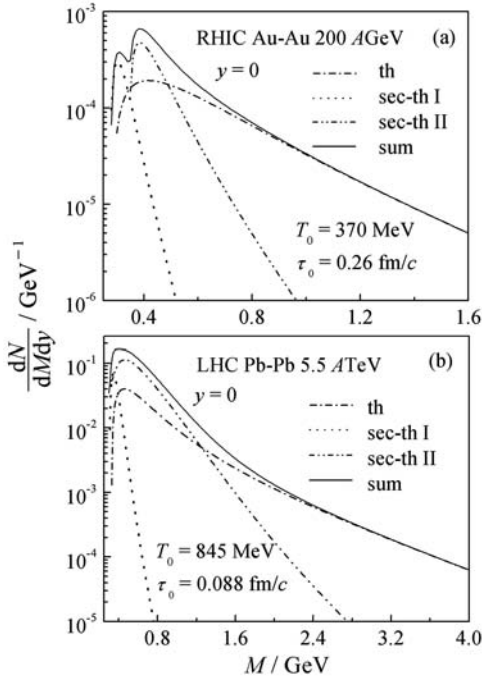


Fig. 1 Thermal dilepton production spectra obtained for Au-Au collisions at RHIC (a) and Pb-Pb collisions at LHC (b).

$0.3 \text{ GeV} < M < 1.2 \text{ GeV}$ for LHC due to the gluon abundance effect at small mass. Then the sec-th dilepton spectra drop rapidly due to the absence of gluon abundance effect in the large mass region of $M > 0.5 \text{ GeV}$ (RHIC) and 1.2 GeV (LHC). Besides, the Color Glass Condensate and Glasma scenarios also support that the gluons are dense at small mass in the heavy ion collisions. In the heavy ion collisions gluons soon become thermal equilibrated and are effectively rescattered [19]. These effective rescattering channels including gluons ensure that the gluon abundance effect is contributing in the secondary parton distributions. In addition, the sum \sum_q in Eq. (7) runs over quark flavors, it makes the scattering channels σ_p having at least 36 choices. The sum also can enhance the contribution of the sec-th production.

In Fig. 1 the sec-th dileptons of the type I are dominant in the mass region of $0.2 \text{ GeV} < M < 0.3 \text{ GeV}$, and the type II is dominant in the mass re-

gion of $0.3 \text{ GeV} < M < 0.5 \text{ GeV}$ at RHIC for Au-Au 200 AGeV collisions. The contribution of sec-th dileptons enhances the spectrum of thermal dileptons in the low mass region of $0.2 \text{ GeV} < M < 0.8 \text{ GeV}$, and the thermal spectrum in this region is almost enhanced by a factor of $1 \sim 3$. In the numerical calculations, we choose the formation time $\tau_0 : 0.26 \text{ fm}/c$ at RHIC [20].

Because the integral range of the time is variable with the initial temperature, the spectrum of the type II which depends on the temperature is changeable with different collision energies. At LHC energy, the spectrum of sec-th dileptons is dominant in the region of $0.3 \text{ GeV} < M < 1.2 \text{ GeV}$. The right panel of Fig. 1 shows that the type II covers the contribution of the type I at LHC, and the spectrum of thermal dileptons is enhanced by the sec-th dileptons in the low mass region of $0.3 \text{ GeV} < M < 1.0 \text{ GeV}$, the enhanced factor is almost $1 \sim 4$. The numerical results also show that the enhancement with a factor of $1 \sim 2$ also exists in the intermediate mass region of $1.0 \text{ GeV} < M < 2.5 \text{ GeV}$. We choose $\tau_0 : 0.088 \text{ fm}/c$ at LHC [20].

From Fig. 2 one can see that the spectrum of dileptons produced from Drell-Yan processes, the

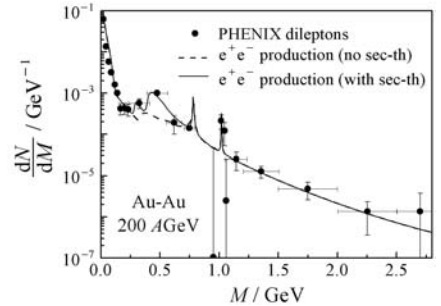


Fig. 2 Dilepton production spectrum (dash line without the secondary thermal contribution [21], solid line with the secondary thermal contribution). Data points are from Ref. [9].

hot medium, the jet-dilepton conversion, and the meson vacuum decays (dash line) [21]. The K factor of the subprocesses of sec-th is used in the calculation for considering the higher-order correction. We use $K : 1.7$ for RHIC and 1.6 for LHC [14]. The higher-order corrections of the dilepton background are also considered in the calculation [21]. The data

points from PHENIX Au-Au 200 AGeV collisions at RHIC are higher than the theory prediction (dash line) in the region of $0.2 \text{ GeV} < M < 0.8 \text{ GeV}$. After considering the secondary thermal contribution the dilepton spectrum is enhanced (solid line). The enhanced factor is almost $2 \sim 3$.

4 Conclusion

The secondary thermal dilepton production is a possible mechanism to interpret the experimental enhancement of the dilepton yield at the low mass. At RHIC energy, the thermal spectrum is enhanced by a factor of $1 \sim 3$ in the mass region of $0.2 \text{ GeV} < M < 0.8 \text{ GeV}$ due to the contribution of the secondary thermal dileptons. The enhancement is more evident in the low mass region of $0.3 \text{ GeV} < M < 1.0 \text{ GeV}$ at LHC, and the enhanced factor is almost $1 \sim 4$. The numerical results show that the enhancement with a factor of $1 \sim 2$ also exists in the intermediate mass region of $1.0 \text{ GeV} < M < 2.5 \text{ GeV}$ at LHC.

References:

- [1] FU Yongping, LI Yunde. Phys Rev C, 2011, **84**: 044906.
 [2] FU Yongping, LI Yunde. Nucl Phys A, 2011, **865**: 76.

- [3] FU Yongping, LI Yunde. Nuclear Physics Review, 2010, **27**: 16.
 [4] AGAKISHIEV G, HADES Collaboration. Phys Rev Lett, 2007, **98**: 052302.
 [5] ARNALDI R, NA60 Collaboration. Phys Rev Lett, 2006, **96**: 162302.
 [6] OZAWA K, ENYO H, FUNAHASHI H, *et al.* Phys Rev Lett, 2001, **86**: 5019.
 [7] ADLER S S, PHENIX Collaboration. Phys Rev C, 2007, **75**: 024909.
 [8] TOIA A, PHENIX Collaboration. Nucl Phys A, 2006, **774**: 743.
 [9] TOIA A, PHENIX Collaboration. Eur Phys J C, 2007, **49**: 243.
 [10] HUNG C M, SHURYAK E V. Phys Rev C, 1997, **56**: 453.
 [11] SRIVASTAVA D K, SINHA B. Phys Rev Lett, 1994, **73**: 2421.
 [12] GALE C, KAPUSTA J I. Nucl Phys B, 1991, **357**: 65.
 [13] GALE C, LICHARD P. Phys Rev D, 1994, **49**: 3338.
 [14] TURBIDE S, GALE C, JEON S, *et al.* Phys Rev C, 2005, **72**: 014906.
 [15] WONG C Y. Introduction to High Energy Heavy-ion Collisions [M]. New York: World Scientific Press, 1994: 205–317.
 [16] RAPP R, SHURYAK E. Phys Lett B, 2000, **473**: 13.
 [17] RUUSKANEN P V. Nucl Phys A, 1992, **544**: 169.
 [18] ALAM J, SRIVASTAVA D K, SINHA B, *et al.* Phys Rev D, 1993, **48**: 1117.
 [19] BERGER E L, BRAATEN E, FIELD R D. Nucl Phys B, 1984, **239**: 52; SHURYAK E, XIONG L. Phys Rev Lett, 1993, **70**: 2241.
 [20] TURBIDE S, GALE C, JEON S, *et al.* Phys Rev C, 2005, **72**: 014906.
 [21] FU Yongping, LI Yunde. Chin Phys Lett, 2010, **27**: 101202;

膨胀 QGP 的热双轻子产生

傅永平¹⁾, 杨光弟, 郝勤

(临沧师范高等专科学校数理系, 云南 临沧 677000)

摘要: 研究了 QGP 中次级热双轻子的产生。在 RHIC 能区, 次级热双轻子的产生在低质量范围 $0.2 \text{ GeV} < M < 0.8 \text{ GeV}$ 内加强了热双轻子谱。次级热双轻子产生机制能够较好地解释 PHENIX Au-Au 200 AGeV 碰撞实验的双轻子增强现象。对于 LHC 能区的 Pb-Pb 5.5 ATeV 碰撞, 理论计算结果表明, 在低质量区域双轻子增强现象会更加明显, 增强区域在 $1.0 \text{ GeV} < M < 2.5 \text{ GeV}$ 范围内。

关键词: 双轻子产生; 次级热双轻子; 相对论重离子碰撞